DOI: http://dx.doi.org/10.22104/jpst.2016.412 Journal of Particle Science and Technology 2 (2016) 103-117

J | P | S | T
jpst.irost.ir

Journal of Particle Science and Technology

IROST

Thin film nanocomposite forward osmosis membrane prepared by graphene oxide embedded PSf substrate

Saharnaz Tajik[1], Omid Moini Jazani[1*], Soheila Shokrollahzadeh[2], Seyed Mahdi Latifi[2]**

[1]*Department of Chemical Engineering, Faculty of Engineering, University of Isfahan, Isfahan, Iran*

[2]*Department of Chemical Technologies, Iranian Research Organization for Science and Technology (IROST), Tehran, Iran*

HIGHLIGHTS

- Novel polysulfone-graphene oxide (PSf-GO) nanocomposite substrates were prepared via phase inversion method for fabrication of thin film nanocomposite forward osmosis (TFN-FO) membranes.
- The existence of functional groups in GO nanoplates increases the substrate hydrophilicity which leads to increase in water permeability of the TFN membranes
- The substrate embedded with 0.5 wt% of GO nanoplates exhibited highest water flux which is the optimum concentration of GO loading.
- Addition of GO nanoplates to the PSf substrate is an effective method to control ICP in FO membranes.

ARTICLE INFO

Article history:
Received 13 August 2016
Received in revised form
16 December 2016
Accepted 19 December 2016

Keywords:
Forward Osmosis (FO)
Nanocomposite Substrates
Graphene Oxide nanoplates
Internal Concentration Polarization (ICP)

GRAPHICAL ABSTRACT

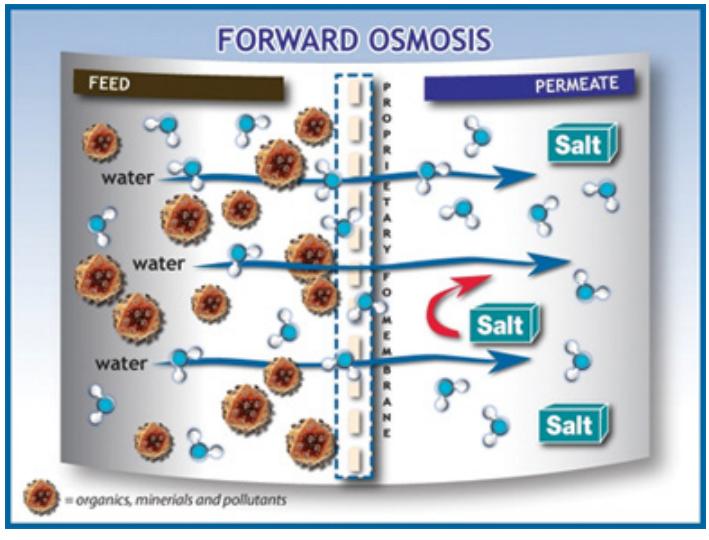

ABSTRACT

One of the limiting factors in good performance of forward osmosis (FO) membranes is the internal concentration polarization (ICP). To reduce ICP, thin film nanocomposite forward osmosis (TFN-FO) membranes were fabricated by adding different amounts of graphene oxide (GO) nanoplates (0-1 wt. %) to polymer matrix of polysulfone (PSf) substrate. The prepared nanocomposite membranes exhibited both hydrophilicity and porosity higher than that of neat PSf counterpart. An optimum amount of 0.5 wt. % was obtained for GO addition into the membranes. The corresponding fabricated thin film nanocomposite (TFN) membrane (TFNG0.5) revealed a water permeability of 2.44 L/m^{2}h bar which is 66% higher compared to an in-house made composite membrane. The FO performance of TFN was assessed by DI water as feed solution and 1 M NaCl as draw solution in AL-DS orientation. The water flux of the synthesized FO membranes increased upon adding of GO nanoplates and reached to a maximum water flux of 37.74 (L/m^{2}h) for TFNG0.5 membrane. This flux is about 3 times higher than TFC membranes without significant changes in their salt rejection. The higher water flux of the TFN membranes can be attributed to ICP decrease originating from reduction of structural parameter of the membranes.

* *Corresponding author. Tel.: +98 31 37934058 ; fax: +98 31 37934037*
E-mail address: o.moini@eng.ui.ac.ir
** *Corresponding author. Tel.: +98 21 56276637 ; fax: +98 21 56276265*
E-mail address: shokrollahzadeh@yahoo.com

1. Introduction

One of the main problems of human society is the shortage of potable water sources that is occurred as a result of rapid population growth and economic development [1]. Membrane technology was introduced as a solution to tackle the crisis of water scarcity through desalination of brackish/salty water with low cost [2-4]. The membrane processes such as reverse osmosis (RO) and nanofiltration (NF) are the most widely methods for seawater desalination and wastewater treatment to product potable water of high quality [5, 6]. The RO is a membrane process in which pure water is obtained by applying hydraulic pressure to the salt solution [7]. In the reverse osmosis process, the hydraulic pressure needed for water transmission across the membrane is directly related to salt concentration. Hence, the high energy consumption, needed to exert high hydraulic pressure, and membrane fouling are the main obstacles to further development of RO process [7, 8].

As a result, researchers in the past few years investigated other possible membrane processes for seawater desalination and wastewater treatment, amongst the forward osmosis (FO) membrane process has attracted a lot of attention as a promising technology due to high fouling resistance and wide range of rejection [9-11]. Unlike RO, FO process utilizes osmotic pressure difference between draw and feed solutions as the driving force for transfer of water across a semi-permeable membrane [2, 12, 13]. In comparison with the pressure-driven membrane processes, it is claimed that FO has potential advantages including lower energy consumption [14, 15], higher water recovery [16, 17], lower fouling tendency and consequently easier cleaning [18-20]. Nevertheless, one of the main problems in FO process is internal concentration polarization (ICP), an unfavorable phenomenon which limits the membrane performance by decreasing the osmotic driving force [21-23]. The ICP is inevitable phenomenon in osmotic driven membrane processes which is based on the membrane orientation. Both concentrative ICP and dilutive ICP can happen in FO processes [24, 25]. In active layer facing the draw solution (AL-DS orientation), a concentrative ICP happens in which the rejected feed solutes accumulate in the support layer of the membrane [26, 27]. In other orientation (active layer facing the feed solution, AL-FS), a dilutive ICP occurs through dilution of the draw solution in support layer by water permeation from feed solution side and aggregation of the feed solutes in the vicinity of the active layer [1, 28]. Therefore, for ICP reduction, the support layer with minimal structural parameter value (S, thickness tortuosity/porosity) is preferred in FO process which leads to a better membrane performance (higher water flux and better solute rejection) [29, 30].

FO membranes with good performance are developed by tailoring their structure [31-34]. In this regard, addition of nanomaterials into the polyamide layer as the membrane substrate is introduced as an effective way to modify the properties and structure of the membrane [27, 28, 35, 36]. By addition of hydrophilic nanomaterials such as titanium dioxide [37], zeolite [38], silica [39], multiwalled carbon nanotubes [40] and graphene oxide modified graphitic carbon nitride [41] into the substrate, FO membranes show improved performance. Due to unique properties, nanomaterials may cause changes in physical-structural properties of the membrane including porosity, hydrophilicity, tensile strength, thermal stability and ICP [42-45].

Emadzadeh et al. [46, 47] investigated the effect of addition of TiO2 nanoparticles into PSf matrix on the membrane performance. They reported that TiO_2 nanoparticles played an important role in water flux due to ICP reduction. Wang et al. [40] fabricated nanocomposite substrate using carbon nanotube for FO applications. They showed that the adding of carbon nanotubes caused changes in the morphology and membrane properties such as porosity, hydrophilicity and structural parameters. Their prepared nanocomposite membranes showed salt rejection over 90%. The presence of zeolite nanoparticles in substrate of FO membranes was also investigated by Ma et al. [38]. The nanocomposite substrates exhibited lower structural parameter and minimal ICP which led to increase in the water flux. Graphene oxide (GO) nanoplates have attracted considerable attention as a filler due to their unique properties such as (1) high specific surface area which creates better interaction with the polymeric support layer; (2) two dimensional nanostructure; (3) high chemical-mechanical stability and (4) excellent hydrophilicity due to existence of oxygenous functional hydrophilic groups such as hydroxyl, carboxyl and carbonyl groups [48-50]. A literature review shows that researchers have utilized GO in preparation of the membranes for different applications. It is confirmed that incorporation of GO improves water flux, enhances salt rejection, increases hydrophilicity and decreases fouling [51-53].

In this study, novel polysulfone-graphene oxide

(PSf-GO) nanocomposite substrates were prepared via phase inversion method for fabrication of thin film nanocomposite forward osmosis (TFN-FO) membranes. The membrane performance is evaluated in terms of water flux, salt rejection, and water/salt permeability. The effects of GO addition on the morphology and structure of the prepared membranes are analyzed by FESEM, AFM and contact angle measurements.

2. Experimental

2.1.Materials

The polysulfone (PSf, Ultrason S 6010) as the polymeric substrate was purchased from BASF Co., Germany. N-methyl-pyrrolidone (NMP, 99.5%, Daejung) and polyvinyl pyrrolidone (PVP-K30, M_w=40,000 g/mol, Daejung) were used as a solvent and a pore former in preparation of the casting solution. The graphene oxide (GO) nanosheets prepared by Staudenmaier method [54] were used for the modification of the substrate properties. M-phenylenediamine (MPD, ≥99%, Acros organics), trimesoyl chloride (TMC, Merck) and n-hexane (>95%, Daejung) were employed to fabricate the PA layer of the membranes. Sodium chloride (NaCl, 99.9%, Pars Namak Co.) was used for the FO tests.

2.2 Preparation of nanocomposite substrates

The flat sheet PSf/GO nanocomposite substrates were prepared using conventional phase inversion method [55]. The casting solution was composed of PSf (12 wt%), PVP (1 wt%) and accurate amounts of GO nanoplates in NMP solvent. The substrates based on their composition are listed in Table 1. Accurate amounts of GO nanoplates (0.1, 0.5 and 1 wt%) were dispersed in NMP using ultrasonication (360 W, 20 kHz, misonix, New York) for 30-45 min (depending on the concentration of GO). Then, PSf and PVP were dissolved in the prepared solution and stirred at 60 °C for 24 h to obtain a homogeneous solution. The polymer solution was degassed degassed to remove air bubbles followed by casting on a clean glass plate using a casting knife with the gate height of 100 μm. The casted polymer solution was immediately immersed in the tap water bath. After few minutes, the formed membrane was separated from the surface glass and washed with deionized water. Finally, the membranes were stored in deionized water bath for 24 h to remove the residual solvent. The membranes were placed between two paper filters for 24 h at room temperature to dry.

2.3. Fabrication of polyamide rejection layer by interfacial polymerization

The PA rejection layer was fabricated on top surface of the PSf and PSf/GO substrates by interfacial polymerization reaction of MPD and TMC monomers. The dried substrate was taped to a glass plate and was immersed in a 2 wt% MPD aqueous solution for 2 min and the excess MPD solution was removed from the substrate surface by a paper filter. The MPD saturated substrate was then soaked in a 0.1 wt. % TMC/n-hexane solution for 1 min. This step is the start of interfacial polymerization reaction which leads to formation of ultrathin PA layer. Finally, the fabricated membranes were washed and stored in deionized water bath at 5 °C. The fabricated membranes with G0, G0.1, G0.5 and G1 substrates were named as TFC, TFNG0.1, TFNG0.5 and TFNG1, respectively.

2.4. Characterization

2.4.1. Characterization of the membranes morphology

The morphologies of the top surface and the cross section of both substrates and TFN membranes were observed by a Field Emission Scanning Electron Microscope (FESEM, JSM-7610F, JEOL). In order to scan cross section, the samples were fractured in liquid nitrogen and were dried for 24 h at room temperature. For imaging, the samples were coated with an ultrathin layer of gold by sputter coater. Atomic Force Microscopy (AFM, DME DualScope 95, Denmark) was used to examine surface morphology and

Table 1.
The composition of PSf substrate matrix.

Substrate type	PSf (wt. %)	PVP (wt. %)	GO nanoplates (wt. %)
G0	12.0	1.0	-
G0.1	12.0	1.0	0.1
G0.5	12.0	1.0	0.5
G1	12.0	1.0	1.0

roughness of the membranes in non-contact mode.

2.4.2. Measurement of contact angle

To investigate the hydrophilicity of the substrate as a function of GO loading, the contact angle of deionized (DI) water placed on the substrate surface was measured by contact angle measuring instrument (G10, KRUSS, Germany). Using sessile drop method, the contact angle (CA) for each sample was measured in 5 random locations and the average value was reported.

2.4.3. Determination of substrate porosity

The overall porosity (ε) of the substrate membrane was calculated by gravimetric method. Initially, dried samples (2 2 cm) were weighed (m_d , g). Then, the samples were immersed in water bath for 24 h. The residual water on the surface of the wet substrate was quickly removed by a clean tissue and the samples were immediately re-weighed (m_w, g). The porosity was calculated by the following equation [34]:

$$\varepsilon = \frac{(m_w - m_d)/\rho_{H_2O}}{(m_w - m_d)/\rho_{H_2O} + m_d/\rho_p} \quad (1)$$

Where ρ_{H_2O} (1.0 g/cm^3) and ρ_p (1.23 g/cm^3) are the densities of water and PSf, respectively.

2.5. Determination of water and salt permeability of the membranes

The water and salt permeability of the fabricated membranes were determined using a dead end filtration unit [30, 32]. The dead end stirred cell volume and effective area were 400 cm^3 and 19.6 cm^2, respectivley. The feed reservoir was pressurized using nitrogen gas. The water permeability (A, L/m^2 h bar) was calculated from the pure water permeation fluxes under pressure of 3 bar.

$$A = \frac{J_w}{\Delta P} \quad (2)$$

Where J_w is the permeate water flux (L/m^2 h) and (bar) is the applied hydraulic pressure [56].

A 2000 mg/L NaCl solution was used for determination of salt permeability. The salt permeability (B, L/m^2 h or m/s) was calculated from the following solution-diffusion theory, where in the salt rejection (R) was determined by conductivity measurement of the both permeate and feed solutions while a conductivity-concentration calibration curve was used. [57].

$$\frac{1-R}{R} = \frac{B}{A(\Delta P - \Delta\pi)} \quad (3)$$

Where A (L/m^2 h bar) is water permeability,ΔP (bar) and Δπ (bar) are pressure difference and osmotic pressure difference, respectively. Also, the salt rejection was calculated as follows:

$$R(\%) = \left(1 - \frac{C_p}{C_f}\right) \times 100 \quad (4)$$

Where C_f (mol/L) and C_p (mol/L) are the salt concentration of the feed and the permeate solutions, respectively [56].

2.6. FO performance of the membranes

The separation performance of the fabricated FO membranes (water flux and salt reverse diffusion) was evaluated using FO lab-scale setup [58] with an effective membrane area of 15.8 cm2. In all experiments, DI water and 1.0 M NaCl solutions were used as the feed and draw solutions, respectively. The membranes were tested in (AL-DS) orientation as active layer faces with the draw solution. The water flux (J_v , L/m^2 h), from the feed solution to the draw solution was calculated (Equation 5) by measuring the volume change of the draw solution during the tests.

$$J_v = \frac{\Delta V_{draw}}{A_m \times \Delta t} \quad (5)$$

In this equation, ΔV_{draw} (L) is the volume change of the draw solution, Δt (h) refers to the time interval and A_m (m^2) is the effective membrane area.
Using a conductometer (LF96, WTW) and applying the conductivity calibration curve, the salt concentration in the feed solution was measured. The salt reverse diffusion (J_s , g/m^2 h) is the salt leakage rate from the draw solution to the feed solution which was calculated by the change of salt concentration in the feed solution.

$$J_s = \frac{V_t.C_t - V_0.C_0}{A_m.\Delta t} \quad (6)$$

The salt leakage rate is calculated through equation 6 where V_0 (L) and V_t(L) are the initial and final volumes of the feed solution, respectively; C_0(mol/L) and C_t(mol/L) are the initial and final salt concentrations of the feed solution, respectively.

2.7. Determination of structural parameter

The structural parameter can be predicated based on the classical model developed by Loeb et al. [26], by the following equations.

In the AL-FS mode (the active layer is facing the feed solution)

$$S = \frac{D}{J_v} \ln \frac{B + A\pi_{D,b}}{B + A\pi_{F,b} + J_v} \quad (7)$$

In the AL-DS mode (the active layer is facing the draw solution)

$$S = \frac{D}{J_v} \ln \frac{B + A\pi_{D,b} - J_v}{B + A\pi_{F,b}} \quad (8)$$

In the aforementioned equations, D (m^2/s) is the solute diffusion coefficient; $\pi_{D,b}$ (bar) and $\pi_{F,b}$ (bar) are the osmotic pressures of the bulk draw and feed solutions, respectively. J_V (L/m^2 h) is also the FO water flux.

3.Results and discussion

3.1. Characterization of the nanocomposite substrates

The effect of adding GO nanoplates on PSf matrix and also its loading on properties and morphology of the fabricated substrates were investigated. The results were compared to the properties and morphology of the pure PSf substrate.

3.1.1. Influence of adding GO nanoplates on the substrate properties

The overall porosity of the composite and nanocomposite substrates prepared in this study was measured and listed in Table 2. As it can be seen, the PSf/GO substrates except G1 have a higher porosity than PSf substrate having no GO nanoplates. Nevertheless, the porosity of all the substrates is in a suitable range (between 74% and 82%), which can be attributed to the low concentration of PSf and PVP additive [59]. The higher porosity of the nanocomposite substrates is due to perch of nanoplates between the intertwined polymer chains which reduces their compaction. Also, the existence of GO hydrophilic nanoplates into the polymer matrix accelerates the phase inversion process and finally leads to thickness decrease of the substrate [60]. However, the results indicate that in high concentrations of GO (more than 0.5 wt%) the substrate porosity is reduced. It is probably due to increased viscosity of the casting solution in high concentrations of GO. As GO concentration exceeds 0.5%, hydrophilicity of the membranes improves significantly and thickness of the substrate increases due to reduced solvent/non-solvent exchange rate. [60, 61]. Zinadini et al. [50] observed the similar behavior for PES/GO membrane.

The hydrophilicity of the membranes is one of the important factors which affects the ICP and water flux, and is evaluated based on water contact angle with the membrane surface [30]. Reducing the contact angle means the hydrophilicity improvement of the prepared membranes. As summarized in Table 2, the contact angle of the substrates first decreases upon adding GO nanoplates to the polymer solution and then increases. Previous studies also demonstrated that adding of hydrophilic nanomaterials into a PSf matrix as fillers increases the substrate hydrophilicity [37, 38, 40, 47, 50, 52]. Pure PSf substrate showed higher contact angle (86°), while the contact angle decreased to 75.1° and 69.8° with adding 0.1 and 0.5 wt% of GO nanoplates, respectively. The increase in hydrophilicity coupled with the decrease in thickness of the nanocomposite substrates (Table 2) may facilitate passage of water molecules through the membranes showing less resistance. This process results in improvement of the membrane performance [37, 62]. Nevertheless, it was observed that the contact angle in high concentration of GO nanoplates (1 wt.%) increased to 72.4° which signifies that high amount of GO addition into the polymer solution does not affect the substrate hydrophilicity positively. It is believed that at high concentrations, GO nanoplates are agglomerated on the surface of the substrate, which leads to reduction in effective surface of the nanoplates as well as reduces population of the functional groups existing on the substrate surface [50, 63].

3.1.2. Influence of GO nanoplates on the substrate morphology

The FESEM images of the top surface and cross section of both composite and nanocomposite substrates are illustrated in Fig. 1. The images of the top surface of the membranes show that the nanocomposite substrates (G0.5 and G1 in Fig. 1(b) and (c))

Table 2
Properties of the synthesized substrates with different concentrations of GO nanoplates.

Substrate	Thickness (μ m)	Porosity (%)	Contact angle (°)
G0	87.19	74.51	86.0
G0.1	85.43	77.91	75.1
G0.5	84.80	82.92	69.8
G1	85.91	75.60	72.4

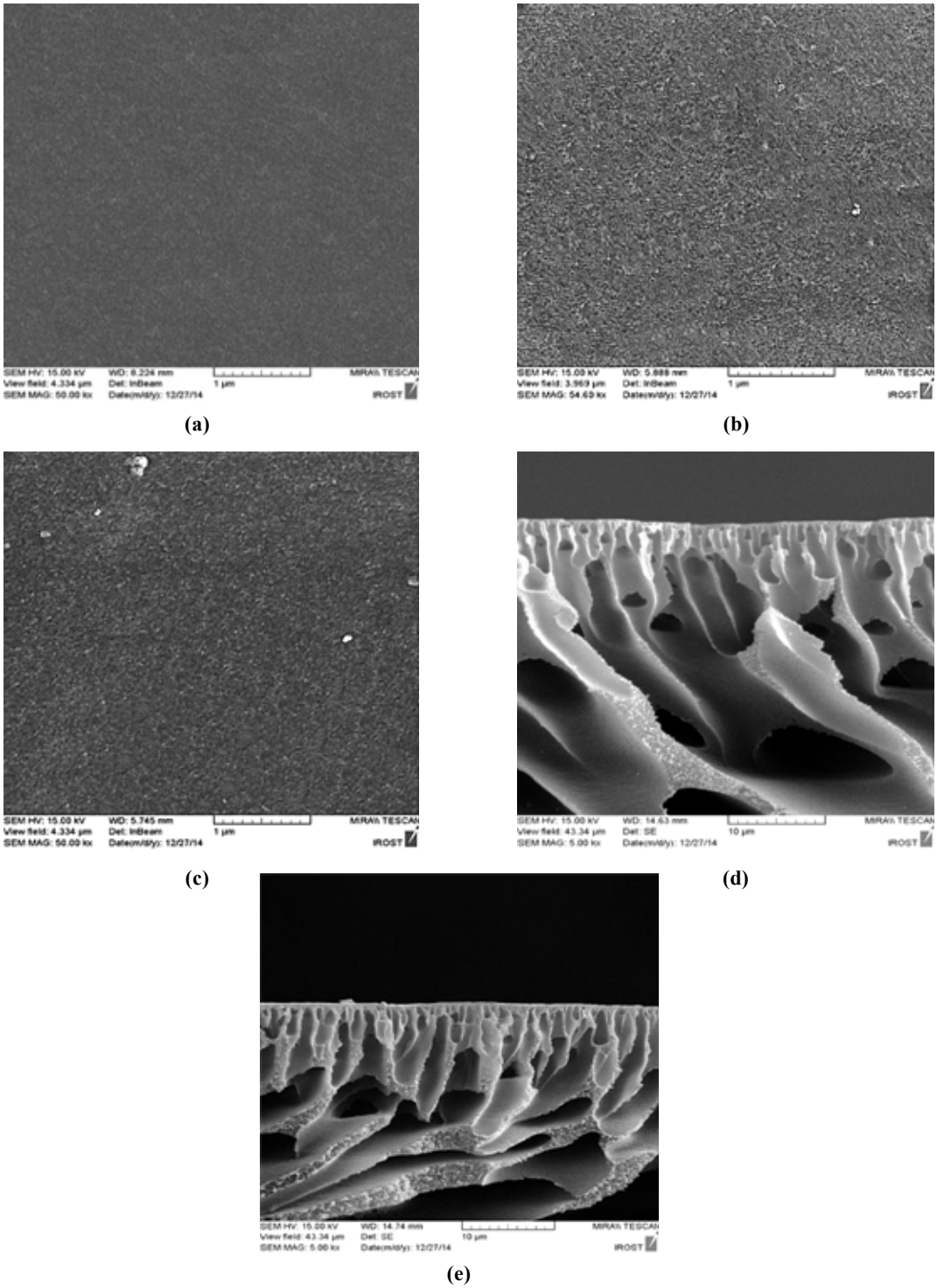

Fig. 1. The FESEM images of PSf substrate and PSf/GO substrates. (a) top surface of the substrate having no GO; (b) top surface of G0.5 substrate; (c) top surface of G1 substrate; (d) cross section of the substrate having no GO, and (e) cross section of G0.5 substrate.

are more porous than PSf substrate having no GO nanoplates. This results are in agreement with the porosity measurements listed in Table 2. The substrates exhibited an asymmetric structure containing a dense top layer and a sublayer with macro voids. The FESEM images show that embedding GO nanoplates in PSf matrix may lead to important changes in the substrate microstructure. As can be seen, the nanocomposite substrates presented longer finger-like structure compared to neat PSf substrate (Fig. 1(d) and (e)) [46].

The difference in morphology of the nanocomposite substrates with the substrate having no GO nanoplates can be originated from increasing rates of solvent (NMP) exit and non-solvent (water) arrival during phase inversion process [51]. It may be expressed that the GO nanoplates, having hydrophilic nature, increases transfer rate of water molecules from water bath to the substrate which ultimately leads to the formation of more finger-like pores and higher overall porosity [41, 64].

Fig. 2 shows digital photos taken from the top and bottom surfaces of G0.5 substrate. As these photos demonstrate, the color of top surface of the nanocomposite substrate is darker than its bottom surface. The reasonable explanation for this phenomenon is that during phase inversion process, GO nanoplates because of high hydrophilicity move toward top surface of the membrane where is the most vulnerable to water [50, 51]. Immigration of GO nanoplates into top surface of the membrane leads to improvement in the substrate hydrophilicity [64].The data obtained from the contact angle measurements (Table 2) support this hypothesis. These results are consistent with previous reports [50, 51, 65]. Also, Vatanpour et al. reported the similar results for carbon nanotube incorporated PES membrane [60, 66].

3.2. Characterization of the fabricated TFC and TFN membranes

3.2.1.Morphology of the TFC/TFN membranes

The FESEM images of the top surface of the TFC and TFNG0.5 membranes are depicted in Fig. 3. The TFC and TFNG0.5 membranes exhibited the ridge-valley surface morphology, which signifies formation of polyamide (PA) layer (through interfacial polymerization between MPD and TMC monomers) on the substrate membrane [36, 62]. Also, comparison of top surface of the TFC and TFNG0.5 membranes (Fig. 3(a) and (b)) displayed enhancing nodular surface of TFN membrane due to presence of GO nanoplates on the surface substrate [39].
According to the cross section images of the membranes (Fig. 3), it seems that polyamide layer formed on the nanocomposite substrates has better adhesion than neat PSf substrate (strong evidences exist in higher magnifications). This is probably due to higher hydrophilicity of the substrates nanocomposite [40]. Hydrophilic groups facilitate better absorption of MPD on the surface and improve its diffusion into pores of the substrates due to existence of interaction between the hydrophilic groups and MPD monomers [40, 62]. Therefore, thinner and deeper polyamide layer is formed within the substrate pores. Based on these results and other research reports, it is offered that the modification of substrate hydrophilicity can be effective method to achieve a PA dense layer from interfacial polymerization, which leads to the improvement of membrane performance [62, 67, 68].

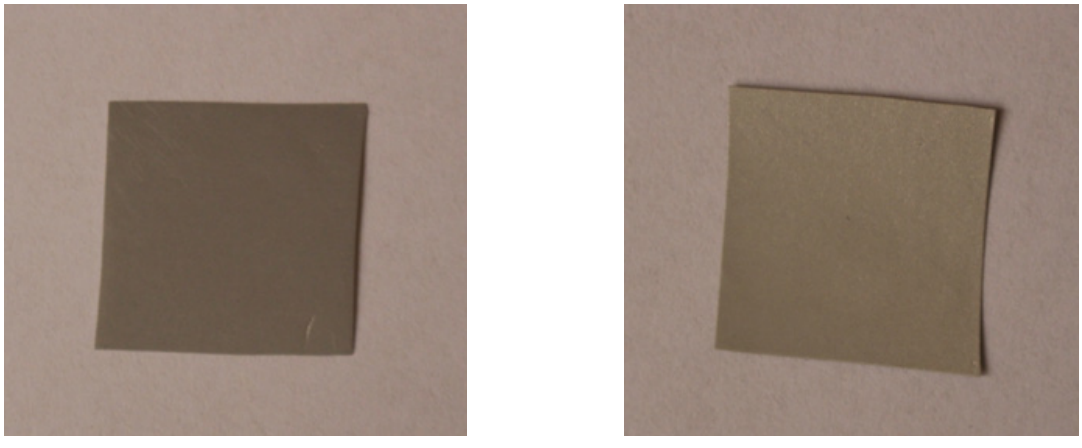

Fig. 2. Digital photographs of the top and bottom surfaces of PSf/GO substrate.

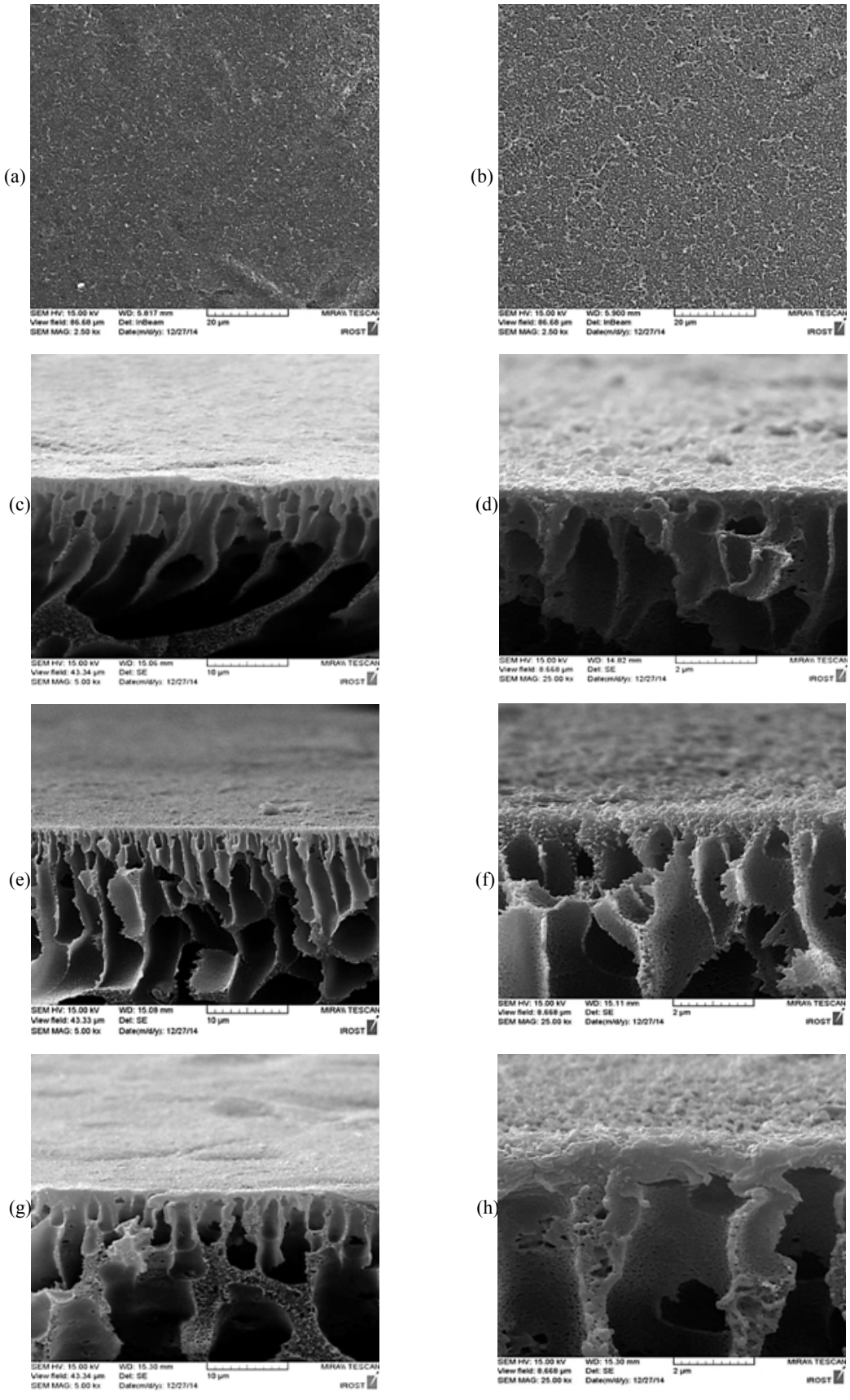

Fig. 3. FESEM images of the TFC/TFN membranes. Top views of (a) TFC; and (b) TFNG0.5 membranes. Cross section views of TFC membrane at low (c) and high (d) magnification; TFNG0.5 membrane at low (e) and high (f) magnification; TFNG1 membrane at low (g) and high (h) magnification.

The previous studies confirmed that physical-chemical characteristics of the substrate membrane and its morphology affect structure and roughness of PA layer prepared by interfacial polymerization [67, 69-71]. Therefore, the surface roughness of all the prepared membranes was examined by AFM images. The three dimensional AFM images taken from PA layer of the nanocomposite and composite membranes are illustrated in Fig. 4. In topographical images, the brightest region reveals the noontide of the membrane surface and the dark zones demonstrate the valleys or membrane pores. The roughness parameters of the membranes surface including the mean roughness (R_a), the root mean square of z valus (R_{ms}) and the maximum vertical distance between the highest data points (R_z) which were calculated using AFM images and SPM DME software in scanning area of 5 5 , are demonstrated in Table 3. It is observed that the surface roughness of the fabricated TFN membranes on the nanocomposite substrates is higher than the TFC membrane. So that, the highest value of roughness parameters belongs to the TFNG0.5 membrane with R_a=36.3 nm, R_{ms}=44.4 nm and R_z=198 nm. The higher surface roughness of the nanocomposite membranes can be ascribed to the nodular of GO nanoplates incorporated in the substrate. These results are in a good agreement with Emadzadeh et al. findings [46]. Also, Ganesh et al. reported that it may occur due to the rapid exchange of solvent and non-solvent during phase inversion process because of the presence of hydrophilic GO nanoplates [51]. However, the subsequent decrease in roughness could be due to the agglomeration of GO nanoplates at high concentrations (> 0.5 wt. %). The increase in surface roughness of TFN membranes significantly facilitates increase of water flux through expansion of the membrane effective area. Hirose et al. reported that a semi-linear relationship exists between water flux and the membrane surface roughness [72].

3.2.2. Water and salt permeability of the prepared membranes

A common method to evaluate the performance of the membranes is the use of a dead end filtration system. By using this system, the water and salt permeability of the prepared membranes were measured and the obtained results are presented in Table 4. As can be observed, all the TFN membranes except TFNG1 exhibited higher water permeability compared to the TFC membrane. So that, the highest value of water permeability was obtained for the TFNG0.5 membrane equal to 2.44 L/m^2 h bar, which is about 1.7 times higher than TFC membrane. The increase of the water permeability of the membranes as a functional of GO loading is due to improvement of hydrophilicity coupled with increase in porosity of the nanocomposite substrates which reduces water diffusion resistance across nanocomposite membrane [38, 40]. Meanwhile, reducing water permeability for TFNG1 membrane can be explained similarly. The results suggest that improving of the substrate properties is an effective method for increasing water permeability of the membrane.

The salt permeability values for TFNG0.1, TFNG0.5 and TFNG1 membranes were reported as 6.31×10^{-7} m/s, 5.81×10^{-7}m/s and 5.97×10^{-7} m/s, respectively. These values are lower than the ones reported for the TFC membranes. This phenomenon can be attributed to the formation of an effective PA layer especially at TFNG0.5 membrane which leads to the increase of salt rejection of the membranes and results in reduced salt permeability. In FO membranes, the lower B/A (water permeability/salt permeability) ratio is favorable, which is indicative of less solute reverse diffusion from draw solution to the feed solution [27, 65]. The TFNG0.5 membrane exhibited lowest B/A value (85.81 kPa). Hence, this membrane has shown maximum separation efficiency.

Table 3
.Surface roughness parameters of TFC and TFN membranes

Membrane	Roughness parameters		
	R_a (nm)	R_{ms} (nm)	R_z (nm)
TFC	20.5	26.0	132
TFNG0.1	26.4	30.0	150
TFNG0.5	36.3	44.4	198
TFNG1	28.3	34.3	161

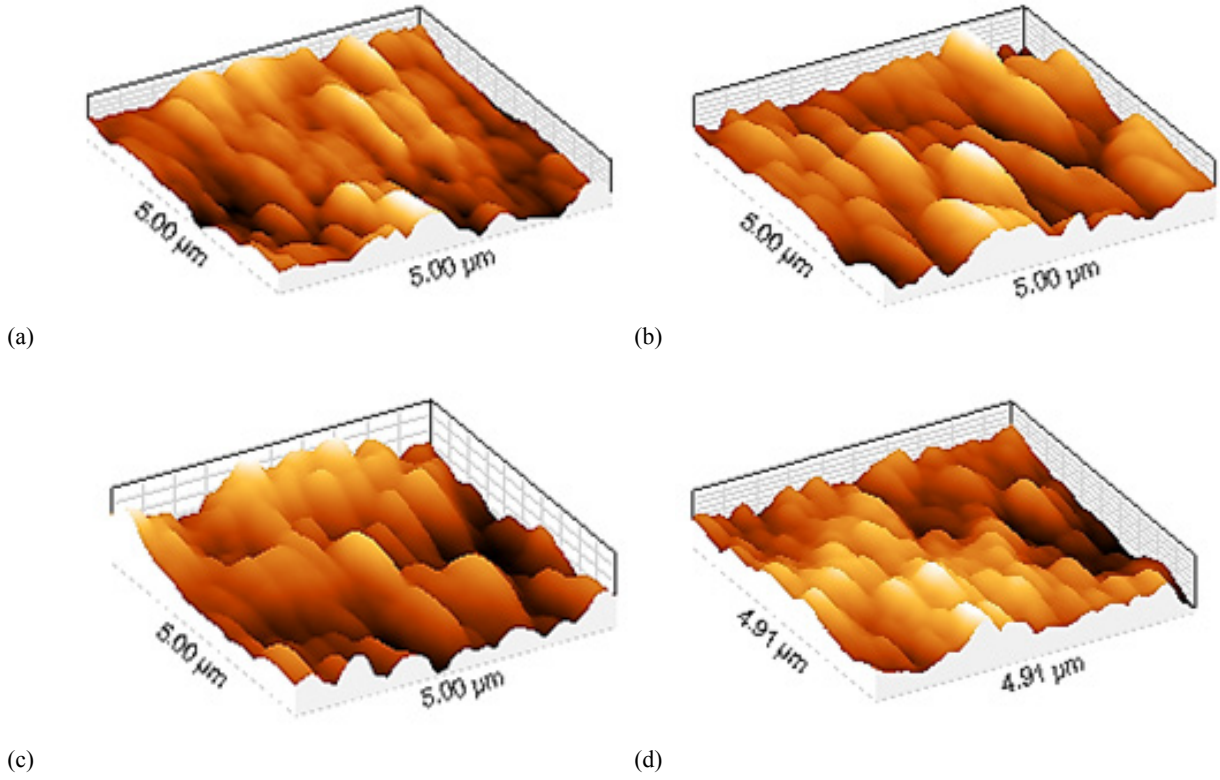

Fig. 4. AFM images of the membranes with different concentrations of GO nanoplates (a) TFC, (b) TFNG0.1, (c) TFNG0.5 and **(d)** TFNG1.

Table 4
Separation properties of prepared TFC and TFN FO membranes.

Membrane	Water permeability A(L/m^2 h bar)	Water permeability A (m/s Pa)	Salt permeability B (m/s)	B/A (kPa)
TFC	1.49	4.13	8.59	207.99
TFNG0.1	1.89	5.25	6.31	120.19
TFNG0.5	2.44	6.77	5.81	85.81
TFNG1	1.97	5.47	5.97	109.14

3.2.3. FO performance of the TFC/TFN membranes

The influence of the nanocomposite substrates containing different amount of GO nanoplates on FO performance of the prepared membranes was investigated and the results were depicted in Fig. 5. The water flux and salt rejection of the membranes were determined using DI water as the feed solution and 1 M NaCl as the draw solution in AL-DS orientation. Clearly, the water flux for all of TFN membranes is higher than the in-house made TFC membrane. This finding is completely consistent with previous reports wherein the prepared TFN membranes containing nanocomposite substrates (containing various nanomaterials such as zeolite, carbon nanotube and titanium dioxide) exhibited higher water flux [37, 38, 40, 46]. The increased water flux indicates that suitable structural changes in the substrate have affected FO performance of the membranes positively [39, 65]. The previous studies proved that the internal concentration polarization (ICP) is extremely effective on FO water flux as it can decrease the water flux to more than 80% during FO process [1, 30, 38]. In current study, the increase in water flux of TFN membranes verifies that substrate modification with GO nanoplates has reduced ICP. This claim is confirmed based on the structural parameter (S) values shown in Fig. 6. Since the structural parameter has an exponential relationship with the ICP, reducing structural parameter leads to the decrease of the ICP and results in better FO membrane performance [73]. Reduction in structural parameter with the increase of GO loading is related to improvement of the properties and structure of nanocomposite substrates [40]. The results

of this study show that the substrate embedded with 0.5 wt% of GO nanoplates exhibited lowest S value (S=0.33 mm) which is the optimum concentration of GO loading. The water flux has shown the compatible trend with S value, when the GO changes. So that, the highest water flux of 37.74 L/m^2 h was achieved for the prepared membrane on G0.5 substrate that is 214% higher than of water flux for TFC membrane. Overall, following reasons can be presented for justifying why TFN membranes compared to TFC ones show higher water flux. (i) The improvement in the morphology and the properties of the substrates upon adding of GO nanoplates, shortens the water diffusion paths and leads to more comfortable transfer of water molecules through membrane and as a result increases water flux [47, 65]. (ii) As GO concentration increases, S value decreases and thereby negative effects arising from ICP are diminished. This phenomenon affects water transfer across the membranes and contributes to an increase of water flux [23, 74]. (iii) The surface roughness enhancement of the PA layer of TFN membranes significantly increases the water flux [72].

The salt rejection of the membranes is also shown in Fig. 5. The salt rejection of the TFN membranes (above 97%) is higher compared to the TFC membrane. The increased salt rejection from 95.63% for TFC membrane to 98.6% for the TFNG0.5 membrane is due to the more adhesive and more perfect formation of PA layer [40]. Nonetheless, a slight decline was observed at salt rejection of the TFNG1 membrane. This result may be due to the agglomeration of GO nanoplates in some locations of the substrate surface which can limit the interfacial polymerization reaction between MPD and TMC monomers and weakens the formation of PA layer and reduces the salt rejection [27, 75].

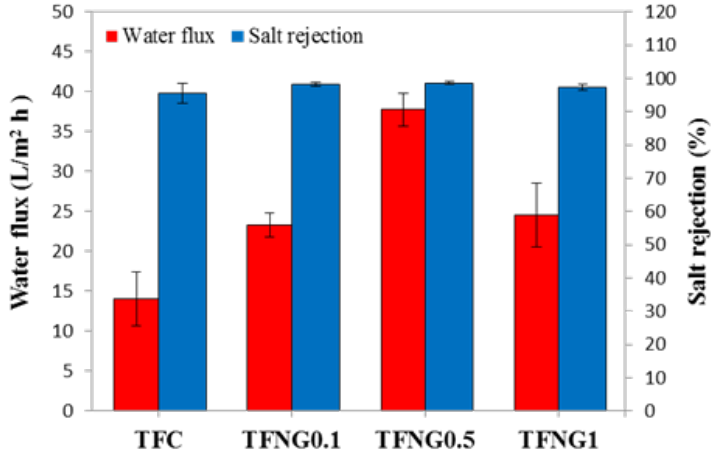

Fig. 5. Comparison of FO water flux and salt rejection of the prepared TFC and TFN membranes.

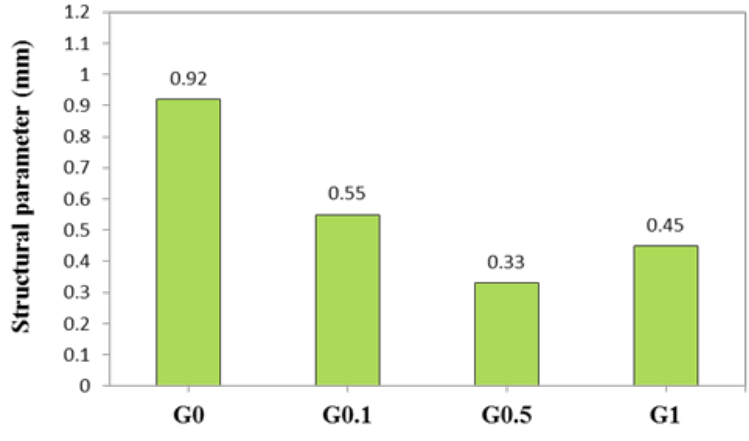

Fig. 6. The structural parameter of the prepared substrates with different loading of GO nanoplates.

4. Conclusions

In the current study, the forward osmosis nanocomposite membranes were prepared therein GO nanoplates were embedded. The effects of GO addition on morphology and performance of the fabricated nanocomposite membranes were investigated. The results demonstrated that the existence of functional groups including hydroxyl, carboxyl and epoxy in GO nanoplates increases the substrate hydrophilicity which leads to increase in water permeability of the TFN membranes. The TFN membranes exhibited higher water flux than TFC one. So that, the water flux increased from 14.09 L/m^2 h for TFC membrane to 37.74 L/m^2 h for TFNG0.5 membrane (i.e. 214% increase). Regarding the achieved results, it was suggested that the optimal concentration of GO nanoplates addition is 0.5 wt. %. The measurements of the substrate structural parameter indicated that with GO loading increment, the S value decreases. This means that addition of GO nanoplates to the PSf substrate is an effective method to control ICP in FO membranes.

Nomenclature & Abbreviations

A	Water permeability coefficient, L/m^2 h bar
A_m	Effective membrane area, m^2
B	Salt permeability coefficient, L/m^2 h (m/s)
C_0	Initial salt concentration of feed solution, mol/L
C_t	Final salt concentration of feed solution, mol/L
C_f	Salt concentration in feed solution, mol/L
C_p	Salt concentration in the permeate solution, mol/L
D	Solute diffusion coefficient, m^2/s
J_s	Salt reverse flux, g/m^2 h
J_w	Water flux in pressure driven process, L/m^2 h
J_v	Water flux in osmotic process, L/m2 h
P	Hydraulic pressure, bar
R	Salt rejection, %
S	Membrane structural parameter, mm
ΔV_{draw}	Volume change of draw solution, L
V_0	Initial volume of feed solution, L
V_t	Final volume of feed solution, L
m_d	Weight of dry membrane, g
m_w	Weight of wet membrane, g
Δt	Operation time interval, h

Greek letters

ε	Membrane porosity, %
π	Osmotic pressure, bar
ρ	Material density, g/cm^3

References

[1] S. Zhao, L. Zou, C.Y. Tang, D. Mulcahy, Recent developments in forward osmosis: Opportunities and challenges, Journal of Membrane Science, 396 (2012) 1-21.

[2] T.-S. Chung, S. Zhang, K.Y. Wang, J. Su, M.M. Ling, Forward osmosis processes: Yesterday, today and tomorrow, Desalination, 287 (2012) 78-81.

[3] H.-S.L.G.M. Geise, D.J. Miller, B.D. Freeman, J.E. Mcgrath, D.R. Paul, Water Purification by Membranes: The Role of Polymer Science, Journal of Polymer Science Part B: Polymer Physics, 48 (2010) 1685-1718.

[4] M.A. Shannon, P.W. Bohn, M. Elimelech, J.G. Georgiadis, B.J. Marinas, A.M. Mayes, Science and technology for water purification in the coming decades, Nature, 452 (2008) 301-310.

[5] M.M. Motsa, B.B. Mamba, A.D. Haese, E.M.V. Hoek, A.R.D. Verliefde, Organic fouling in forward osmosis membranes: The role of feed solution chemistry and membrane structural properties, Journal of Membrane Science, 460 (2014) 99-109.

[6] C. Charcosset, A review of membrane processes and renewable energies for desalination, Desalination, 245 (2009) 214-231.

[7] J. Dong, L. Li, T.M. Neoff, R. Lee, Desalination by reverse osmosis using MFI zeolite membranes, journal of Membrane Science, 243 (2004) 401-404.

[8] D. Mattai, K.P. Lee, T.C. Arnot, A review of reverse osmosis membrane materials for desalination – development to date and future potential, Journal of Membrane Science, 370 (2011) 1-22.

[9] O.A. Bamaga, A. Yokochi, B. Zabara, A.S. Babaqi, Hybrid FO/RO desalination system: preliminary assessment of osmotic energy recovery and designs of new FO membrane module configuration, Desalination, 268 (2011) 163-169.

[10] M. Elimelech, W.A. Phillip, The future of seawater desalination: energy, technology, and the environment, Science, 333 (2011) 712-717.

[11] E.M.V. Hoek, M.C.Y. Wong, K. Martinez, G.Z. Ramon, Impacts of operating conditions and solution chemistry on osmotic membrane structure and performance, Desalination, 287 (2012) 340-349.

[12] J.R. McCutcheon, R.L. McGinnis, M. Elimelech, Desalination by ammonia–carbon dioxide forward osmosis: Influence of draw and feed solution concentrations on process performance, Journal of Membrane

Science, 278 (2006) 114-123.
[13] C. Suh, S. Lee, Modeling reverse draw solute flux in forward osmosis with external concentration polarization in both sides of the draw and feed solution, Journal of Membrane Science 427 (2013) 114-123.
[14] Z. Liu, H. Bai, J. Lee, D.D. Sun, A low-energy forward osmosis process to produce drinking water, Energy & Environmental Science 4(2011) 2582.
[15] R.L. McGinnis, M. Elimelech, Energy requirements of ammonia–carbon dioxide forward osmosis desalination, Desalination, 207 (2007) 370-382.
[16] C.R. Martinetti, A.E. Childress, T.Y. Cath, High recovery of concentrated RO brines using forward osmosis and membrane distillation, Journal of Membrane Science, 331 (2009) 31-39.
[17] S. Zhao, L. Zou, Effects of working temperature on separation performance, membrane scaling and cleaning in forward osmosis desalination, Desalination, 278 (2011) 157-164.
[18] A. Achilli, T.Y. Cath, E.A. Marchand, A.E. Childress, The forward osmosis membrane bioreactor: a low fouling alternative to MBR processes, Desalination, 239 (2009) 10-21.
[19] S. Lee, C. Boo, M. Elimelech, S. Hong, Comparison of fouling behavior in forward osmosis (FO) and reverse osmosis (RO), Journal of Membrane Science 365 (2010) 34-39.
[20] B. Mi, M. Elimelech, Organic fouling of forward osmosis membranes: Fouling reversibility and cleaning without chemical reagents, Journal of Membrane Science, 348 (2010) 337-345.
[21] Y. Gao, Y.-N. Wang, W. Li, C.Y. Tang, Characterization of internal and external concentration polarizations during forward osmosis processes, Desalination, 338 (2014) 65-73.
[22] J.R. McCutcheon, R.L. McGinnis, M. Elimelech, A novel ammonia-carbon dioxide forward (direct) osmosis desalination process, Desalination, 174 (2005) 1-11.
[23] C.Y. Tang, Q. She, W.C.L. Lay, R. Wang, A.G. Fane, Coupled effects of internal concentration polarization and fouling on flux behavior of forwar dosmosis membranes during humic acid filtration, Journal of Membrane Science 354 (2010) 123-133.
[24] G.T. Gray, J.R. McCutcheon, M. Elimelech, Internal concentration polarization in forward osmosis" role of membrane orientation, Desalination, 197 (2006) 1-8.
[25] J.R. McCutcheon, M. Elimelech, Influence of concentrative and dilutive internal concentration polarization on flux behavior in forward osmosis, Journal of Membrane Science, 284 (2006) 237-247.
[26] S. Loeb, L. Titelman, E. Korngold, J. Freiman, Effect of porous support fabric on osmosis through a Loeb-Sourirajan type asymmetric membrane, Journal of Membrane Science, 129 (1997) 243-249.
[27] N. Niksefat, M. Jahanshahi, A. Rahimpour, The effect of SiO_2 nanoparticles on morphology and performance of thin film composite membranes for forward osmosis application, Desalination, 343 (2014) 140-146.
[28] M. Amini, M. Jahanshahi, A. Rahimpour, Synthesis of Novel Thin Film Nanocomposite (TFN) Forward Osmosis Membranes Using Functionalized Multi-walled Carbon Nanotubes, Journal of Membrane Science, 435 (2013) 233-241.
[29] N.-N. Bui, M.L. Lind, E.M.V. Hoek, J.R. McCutcheon, Electrospun nanofiber supported thin film composite membranes for engineered osmosis, Journal of Membrane Science, 385-386 (2011) 10-19.
[30] J.M.C. Puguan, H.-S. Kim, K.-J. Lee, H. Kim, Low internal concentration polarization in forward osmosis membranes with hydrophilic crosslinked PVA nanofibers as porous support layer, Desalination, 336 (2014) 24-31.
[31] Y.H. Cho, J. Han, S. Han, M.D. Guiver, H.B. Park, Polyamide Thin-Film Composite Membranes Based on Carboxylated Polysulfone Microporous Support Membranes for Forward Osmosis, Journal of Membrane Science, 445 (2013) 220-227.
[32] G. Han, S. Zhang, X. Li, N. Widjojo, T.-S. Chung, Thin film composite forward osmosis membranes based on polydopamine modified polysulfone substrates with enhancements in both water flux and salt rejection, Chemical Engineering Science, 80 (2012) 219-231.
[33] N. Widjojo, T.-S. Chung, M. Weber, C. Maletzko, V. Warzelhan, The role of sulphonated polymer and macrovoid-free structure in the support layer for thin-film composite (TFC) forward osmosis (FO) membranes, Journal of Membrane Science, 383 (2011) 214-223.
[34] N. Widjojo, T.-S. Chung, M. Weber, C. Maletzko, V. Warzelhan, A sulfonated polyphenylenesulfone (sPPSU) as the supporting substrate in thin film composite (TFC) membranes with enhanced performance for forward osmosis (FO), Chemical Engineering Journal, 220 (2013) 15-23.
[35] G.L. Jadav, P.S. Singh, Synthesis of novel silica-polyamide nanocomposite membrane with enhanced properties, Journal of Membrane Science, 328 (2009) 257-267.
[36] N. Ma, J. Wei, R. Liao, C.Y. Tang, Zeolite-polyamide thin film nanocomposite membranes: Towards enhanced performance for forward osmosis, Journal of Membrane Science, 405-406 (2012) 149-157.
[37] D. Emadzadeh, W.J. Lau, T. Matsuura, M. Rahbari-Sisakht, A.F. Ismail, A novel thin film composite

forward osmosis membrane prepared from PSf–TiO2 nanocomposite substrate for water desalination, Chemical Engineering Journal, 237 (2014) 70-80.
[38] N. Ma, J. Wei, S. Qi, Y. Zhao, Y. Gao, C.Y. Tang, Nanocomposite substrates for controlling internal concentration polarization in forward osmosis membranes, Journal of Membrane Science, 441 (2013) 54-62.
[39] X. Liu, H.Y. Ng, Fabrication of layered silica–polysulfone mixed matrix substrate membrane for enhancing performance of thin-film composite forward osmosis membrane, journal of Membrane Science, 481 (2015) 148-163.
[40] Y. Wang, R. Ou, Q. Ge, H. Wang, T. Xu, Preparation of polyethersulfone/carbon nanotube substrate for high-performance forward osmosis membrane, Desalination, 330 (2013) 70-78.
[41] Y. Wang, R. Ou, H. Wang, T. Xu, Graphene oxide modified graphitic carbon nitride as a modifier for thin film composite forward osmosis membrane, Journal of Membrane Science, (2014).
[42] J.H. Choi, J. Jegal, W.N. Kim, Fabrication and characterization of multi-walled carbon nanotubes/polymer blend membranes, Journal of Membrane Science, 284 (2006) 406-415.
[43] Y. Jia, H. Li, M. Wang, L. Wu, Y. Hu, Carbon nanotube: Possible candidate for forward osmosis, Separation and Purification Technology, 75 (2010) 55-60.
[44] E.S. Kim, G. Hwang, M.G. El-Din, Y. Liu, Development of nanosilver and multiwalled carbon nanotubes thin-film nanocomposite membrane for enhanced water treatment, Journal of Membrane Science, 394–395 (2011) 37–48.
[45] A. Rahimpour, M. Jahanshahi, S. Khalili, A. Mollahosseini, A. Zirepour, B. Rajaeian, Novel functionalized carbon nanotubes for improving the surface properties and performance of polyethersulfone (PES) membrane, Desalination, 286 (2011) 99–107.
[46] D. Emadzadeh, W.J. Lau, A.F. Ismail, Synthesis of thin film nanocomposite forward osmosis membrane with enhancement in water flux without sacrificing salt rejection, Desalination 330 (2013) 90-99.
[47] D. Emadzadeh, W.J. Lau, T. Matsuura, A.F. Ismail, M. Rahbari-Sisakht, Synthesis and characterization of thin film nanocomposite forward osmosis membrane with hydrophilic nanocomposite support to reduce internal concentration polarization, Journal of Membrane Science, 449 (2014) 74-85.
[48] C. Lee, X.D. Wei, J.W. Kysar, J. Hone, Measurement of the elastic properties and intrinsic strength of monolayer graphene, Science, 321 (2008) 385-388.
[49] H. Wu, B. Tang, P. Wu, Development of novel SiO_2-GO nanohybrid/polysulfone membrane with enhanced performance Journal of Membrane Science, 451 (2014) 94-102.
[50] S. Zinadini, A.A. Zinatizadeh, M. Rahimi, V. Vatanpour, H. Zangeneh, Preparation of a novel antifouling mixed matrix PES membrane by embedding graphene oxide nanoplates, Journal of Membrane Science, 453 (2014) 292-301.
[51] B.M. Ganesh, A.M. Isloor, A.F. Ismail, Enhanced hydrophilicity and salt rejection study of graphene oxide-polysulfone mixed matrix membrane, Desalination, 313 (2013) 199-207.
[52] Z. Xu, J. Zhang, M. Shan, Y. Li, B. Li, J. Niu, B. Zhou, X. Qian, Organosilane-functionalized graphene oxide for enhanced antifouling and mechanical properties of polyvinylidene fluoride ultrafiltration membranes, Journal of Membrane Science, 458 (2014) 1-13.
[53] H. Zhao, L. Wu, Z. Zhou, L. Zhang, H. Chen, Improving the antifouling property of polysulfone ultrafiltration membrane by incorporation of isocyanate-treated graphene oxide, Physical chemistry chemical physics : PCCP, 15 (2013) 9084-9092.
[54] S. Sheshmani, M.A. Fashapoyeh, Suitable chemical methods for preparation of graphene oxide, graphene and surface functionalized graphene nanosheets, Acta Chimica Slovenica, 60 (2014) 813-825.
[55] B. Chakrabarty, A.K. Ghoshal, M.K. Purkait, Preparation, characterization and performance studies of polysulfone membranes using PVP as an additive, Journal of Membrane Science, 315 (2008) 36-47.
[56] T.Y. Cath, A.E. Childress, M. Elimelech, Forward osmosis: principles, applications, and recent developments, Journal of Membrane Science, 281 (2006) 70-87.
[57] S. Loeb, G.D. Mehta, A two-coefficient water transport equation for pressure-retarded osmosis, Journal of Membrane Science, 4 (1979) 351-362.
[58] E.R. Cornelissen, D. Harmsen, K.F.d. Korte, C.J. Ruiken, J.-J. Qin, H. Oo, L.P. Wessels, Membrane fouling and process performance of forward osmosis membranes on activated sludge, Journal of Membrane Science, 319 (2008) 158-168.
[59] E. Yuliwati, A.F. Ismail, Effect of additives concentration on the surface properties and performance of PVDF ultrafiltration membranes for refinery produced wastewater treatment, Desalination, 273 (2011) 226-234.
[60] V. Vatanpour, S.S. Madaeni, R. Moradian, S. Zinadini, B. Astinchap, Fabrication and characterization of novel antifouling nanofiltration membrane prepared from oxidized multiwalled carbon nanotube/polyethersulfone nanocomposite, Journal of Membrane Science, 375 (2011) 284-294.
[61] S. Qiu, L. Wu, X. Pan, L. Zhang, H. Chen, C. Gao,

Preparation and properties of functionalized carbon nanotube/PSF blend ultrafiltration membranes, Journal of Membrane Science, 342 (2009) 165-172.
[62] M. Fathizadeh, A. Aroujalian, A. Raisi, Effect of lag time in interfacial polymerization on polyamide composite membrane with different hydrophilic sub layers, Desalination, 284 (2012) 32-41.
[63] E. Celik, H. Park, H. Choi, H. Choi, Carbon nanotube blended polyethersulfone membranes for fouling control in water treatment, Water Research, 45 (2011) 274-282.
[64] J. Lee, H.-R. Chae, Y.J. Won, K. Lee, C.-H. Lee, H.H. Lee, I.-C. Kim, J.-m. Lee, Graphene oxide nanoplatelets composite membrane with hydrophilic and antifouling properties for wastewater treatment, Journal of Membrane Science, 448 (2013) 223-230.
[65] M.J. Park, S. Phunstho, T. He, G.M. Nisola, L.D. Tijing, X.-M. Li, G. Chen, W.-J. Chung, H.K. Shon, Graphene oxide incorporated polysulfone substrate for the fabrication of flat sheet thin-film composite forward osmosis membranes.
[66] V. Vatanpour, S.S. Madaeni, R. Moradian, S. Zinadini, B. Astinchap, Novel antibifouling nanofiltration polyethersulfone membrane fabricated from embedding TiO2 coated multiwalled carbon nanotubes, Separation and Purification Technology, 90 (2012) 69-82.
[67] A.K. Ghosh, E.M.V. Hoek, Impacts of support membrane structure and chemistry on polyamide–polysulfone interfacial composite membranes, Journal of Membrane Science, 336 (2009) 140-148.
[68] H.I. Kim, S.S. Kim, Plasma treatment of polypropylene and polysulfone supports for thin film composite reverse osmosismembrane, journal of Membrane Science, 286 (2006) 193-201.
[69] L. Shi, S.R. Chou, R. Wang, W.X. Fang, C.Y. Tang, A.G. Fane, Effect of substrate structure on the performance of thin-film composite forward osmosis hollow fiber membranes, Journal of Membrane Science, 382 (2011) 116-123.
[70] P.S. Singh, S.V. Joshi, J.J. Trivedi, C.V. Devmurari, A.P. Rao, P.K. Ghosh, Probing the structural variations of thin film composite RO membranes obtained by coating polyamide over polysulfone membranes of different pore dimensions, Journal of Membrane Science, 278 (2006) 19-25.
[71] X. Liu, H.Y. Ng, Double-blade casting technique for optimizing substrate membrane in thin-film composite forward osmosis membrane fabrication, Journal of Membrane Science, 469 (2014) 112-126.
[72] M. Hirose, H. Ito, Y. Kamiyama, Effect of skin layer surface structures on the flux behaviour of RO membranes, Journal of Membrane Science, 121 (1996) 209-215.
[73] W.C.L. Lay, J. Zhang, C. Tang, R. Wang, Y. Liu, A.G. Fane, Factors affecting flux performance of forward osmosis systems, Journal of Membrane Science, 394 (2012) 151-168.
[74] K.L. Lee, R.W. Baker, H.K. Lonsdale, Membranes for power generationby pressure-retarded osmosis, Journal of Membrane Science, 8 (1981) 141-171.
[75] J. Jegal, S.G. Min, K.-H. Lee, Factors affecting the interfacial polymerization of polyamide active layers for the formation of polyamide composite membranes, Journal of Applied Polymer Science 86 (2002) 2781-2787.